# Synergistic Kinetic Interactions between Components of the Phosphorelay Controlling Sporulation in *Bacillus subtilis*†

Charles E. Grimshaw,‡ Shaoming Huang,§ Conrad G. Hanstein, Mark A. Strauch, David Burbulys,‡ Ling Wang,‡ James A. Hoch, and John M. Whiteley*

*The Scripps Research Institute, R. W. Johnson Pharmaceutical Research Institute, La Jolla, California 92037*

*Received August 4, 1997; Revised Manuscript Received October 14, 1997*

ABSTRACT: The four individual phosphotransfer steps in the multicomponent phosphorelay system controlling sporulation in *Bacillus subtilis* have been characterized kinetically using highly purified samples of the individual protein components *in vitro*. The autophosphorylation of KinA is the initial occurrence, and a divalent metal ion is required. KinA-mediated phosphotransfer, which displays a 57000-fold preference ($k_{cat}/K_m$) for catalysis of Spo0F-P formation relative to Spo0A-P formation, is shown to proceed via a hybrid ping-pong/sequential mechanism with pronounced (≥40-fold) substrate synergism by Spo0F of KinA autophosphorylation. In addition, evidence is presented for formation of an abortive KinA·Spo0F complex. Kinetic parameters derived for Spo0F-P and Spo0A as substrates for Spo0B, the second phosphotransferase in the phosphorelay chain, indicate that Spo0B-mediated production of Spo0A-P is 1.1-million-fold more efficient ($k_{cat}/K_{Spo0A}$) than the direct KinA-mediated process. A rationale is presented for a four component cascade as the means for controlling sporulation, which focuses on the utility of synergistic interactions among the phosphorelay components that may be modulated by environmental stimuli.

A variety of prokaryotic transcription activation systems have now been identified that operate via a histidine protein kinase that autophosphorylates in response to an environmental stimulus and catalyzes transfer of the terminal phosphate of ATP to an aspartyl group of a specific "response regulator" protein which can then modulate expression of certain genes (*1*). In most cases there are only two components, a histidine protein kinase and a response regulator/transcription activator substrate. A more complex system is found in *Bacillus subtilis*, however, where the process of sporulation is controlled by a phosphorelay comprised of not only the standard kinase (KinA) or alternate kinase (KinB) and response regulator (Spo0A), but at least two additional components, Spo0F and Spo0B. Previously, it has been shown that the flow of phosphate from ATP proceeds most efficiently via the pathway shown in the following scheme:

Signal transduction

$$\text{ATP} + \text{KinA} \leftrightarrow \text{ADP} + \text{KinA}\sim\text{P}$$

Phosphotransfer

$$\text{KinA}\sim\text{P} + \text{Spo0F} \leftrightarrow \text{KinA} + \text{Spo0F}\sim\text{P}$$

Phosphotransfer

$$\text{Spo0F}\sim\text{P} + \text{Spo0B} \leftrightarrow \text{Spo0F} + \text{Spo0B}\sim\text{P}$$

Phosphotransfer

$$\text{Spo0B}\sim\text{P} + \text{Spo0A} \leftrightarrow \text{Spo0B} + \text{Spo0A}\sim\text{P}$$

The phosphorelay is now known to utilize two kinases (KinA and KinB) as phosphate donors (*5*). The relative activities of these enzymes depend on environmental conditions, and the effecter molecules sensed by the kinases that directly interact with and control their activity have not been discovered. However, one kinase, KinA, is at least partially regulated by a protein inhibitor of catalysis that is, in turn, regulated by the availability of fixed nitrogen (*6*). Regulation of the kinases is only one means by which this pathway is controlled. The phosphorylated active form of the Spo0A transcription factor is subject to deactivation by the Spo0E phosphatase (*7*). Several members of a family of Rap phosphatases control the phosphorylated state of Spo0F and thereby the level of active phosphorylated Spo0A transcription factor (*8*−*10*). Expression of the phosphatases is transcriptionally controlled and their activity is regulated by peptides (*11*). Since sporulation initiation is absolutely

† This investigation was supported in part by Grants GM45724 (J.M.W.) and GM19416 (J.A.H.) from the National Institutes of Health and the Sam and Rose Stein Charitable Trust (TSRI). This is publication 11028-MEM from the Department of Molecular and Experimental Medicine at The Scripps Research Institute.

* Correspondence should be addressed to Department of Molecular and Experimental Medicine, NX-2, The Scripps Research Institute, 10550 North Torrey Pines Road, La Jolla, CA 92037. Fax: 619 784-7981. E-mail: jmw@scripps.edu.

‡ Current address: IGEN International, Gaithersburg, MD 20877 (C.E.G.); UCLA School of Medicine, Torrance, CA 90509 (D.B.); Nanogen, Inc., San Diego, CA 92121 (L.W.).

§ R. W. Johnson Pharmaceutical Research Institute.

S0006-2960(97)01917-X CCC: $15.00 
Published on Web 02/03/1998

dependent on the functioning of this transcription factor, these controls and others yet to be discovered on this signal transduction system make the phosphorelay a signal integration circuit that allows many environmental, metabolic, and cell cycle signals to impact on the decision to sporulate (*7*, *12*). Moreover, the inclusion of Spo0B in the overall process provides a means whereby the *B. subtilis* cell can integrate additional input from environmental stimuli in order to avoid any spurious commitment to the energy-intensive process of spore formation (*13*). In order to understand the basis for control of this elegant phosphorelay system, the kinetic properties of each of the steps along the pathway using highly purified preparations of the individual components have been characterized. The results presented detail marked synergy in the catalysis of phosphoryl transfer resulting from interactions among the various components. Few kinetic analyses of the two component regulatory systems have been reported (*14*−*18*), and similarities to these systems are noted, as are the unique properties of the sporulation phosphorelay.

## MATERIALS AND METHODS

*B. subtilis* Spo0F, Spo0B, and Spo0A were purified from pKQV4 strains of *Escherichia coli* by procedures published elsewhere (*19*−*21*). The recombinant proteins were determined to be homogeneous by HPLC and SDS−PAGE analysis. Unless otherwise noted, all chemicals and biochemicals were obtained from Sigma Chemical Co., St. Louis, MO. The concentration of Spo0F was determined using the extinction coefficient ($\epsilon_{275nm}$ = 7000 $M^{-1}$ $cm^{-1}$) and by the Bradford dye binding assay with bovine serum albumin as the standard (*22*). The concentrations of the other protein components were routinely estimated by the latter procedure. Absolute stoichiometries of the various phosphorylated reaction components could be determined (see below) by running the phosphotransfer reaction to completion using purified [$\gamma$-$^{32}$P] and using [$^{32}$-P]Spo0F-P as the internal standard.

*SDS−Polyacrylamide Gel Electrophoresis.* The procedure was carried out according to the method of Laemmli (*23*) on gels (8 × 4 × 0.075 cm) using bovine serum albumin ($M_r \approx$ 66 000), ovalbumin ($M_r \approx$ 45 000), and α-lactalbumin ($M_r \approx$ 14 200) as standards. Proteins were separated on 15% gels.

*KinA Purification. E. coli* strain DH5α, harboring the plasmid pJM8118, was grown at 37 °C with shaking (170 rpm) in Luria-Bertani medium containing ampicillin (100 $\mu$g/mL). When the cells reached an $OD_{595}$ of 0.5, the incubation temperature was reduced to 30 °C and shaking (220 rpm) was continued for 1 h. At this time, the cells were induced with IPTG[1] (Diagnostic Chemicals Limited) to a final concentration of 0.2 mM, and incubation was continued overnight (21−22 h). The cells were harvested by centrifugation (10 800*g*) for 10 min, 4 °C. The cell pellet was washed once with buffer A [25 mM Tris, pH 8.0 (4 °C), 10 mM KCl, and 1 mM EDTA] and placed at −20 °C overnight. The cell pellet was resuspended in 4−5 mL of buffer B (buffer A with 5 mM $\beta$-ME and 1 mM PMSF)/g (wet weight) of cell pellet. The cell suspension was placed in a rosette flask on ice and sonicated (Heat Systems-Ultrasonics, Inc. sonicator model W-220F) on setting 8 with three 1 min bursts and 2 min rests. Complete lysis was determined microscopically. The cell lysate was centrifuged at 26 900*g*, 40 min, 4 °C, and the supernatant containing soluble KinA was carefully decanted and its volume determined. Saturated ammonium sulfate (4.1 M at 25 °C) was added dropwise while stirring on ice to 35%. After an additional 20 min of stirring, the suspension was centrifuged 23400*g* for 1 h, 4 °C. The KinA containing pellet was resuspended with 10−12 mL of buffer B/g of (wet weight) of pellet. The suspension was dialyzed against 2 L of buffer B using 6−8K MWCO Spectra/Por dialysis tubing (Spectrum) for 2 h, and one buffer change was made overnight.

The dialysate was centrifuged to remove any precipitated material 11950*g* for 10 min, 4 °C, and was loaded (1 mL/min) onto a Bio-Rad Affi-Gel Blue column (2.5 × 8.5 cm) equilibrated with buffer C (buffer A containing 5 mL of $\beta$-ME). The column was washed with buffer C until $OD_{280}$ approached baseline. KinA was then eluted with buffer C containing 1 M KCl and fractions containing KinA, determined by SDS−PAGE, were pooled and dialyzed against 4 L of buffer C overnight. The dialysate was centrifuged as before and was loaded (1 mL/min) onto a Pharmacia HiLoad 16/10 Q-Sepharose High Performance (HP) column (1.6 × 10 cm). The column was washed with 200 mM KCl in buffer C (2 mL/min) until $OD_{280}$ approached baseline. KinA was eluted by a 250 mL linear gradient of 200 to 350 mM KCl in buffer C. KinA fractions characterized by SDS−PAGE were pooled and centrifuged in a Centriprep 30 concentrator (Amicon) 1460*g* until concentrated to 3−4 mL.

The concentrated KinA was loaded (1 mL/min) onto a Pharmacia Sephacryl S-300 high resolution column (2.5 × 95 cm) equilibrated in buffer D (50 mM Tris, pH 8.0, 50 mM KCl, and 5 mM $\beta$-ME). Homogeneous KinA was eluted and detected by SDS−PAGE. Routinely, an ATPase assay is performed on the fractions using a coupled reaction of pyruvate kinase and lactate dehydrogenase (*24*). The activities of the fractions are determined by measuring the decrease of $OD_{340}$. Fractions with low ATPase activity are pooled and concentrated in a Centriprep 30 as before and dialyzed into storage buffer (50 mM Tris, pH 8.0, 1 mM DTT, and 40% glycerol) at 4 °C overnight. KinA is then stored at −20 °C and remains stable indefinitely under these conditions.

*KinA-Mediated Autophosphorylation and Phosphotransfer Assays.* The standard fixed time point assay mixture (40 $\mu$L total volume) contained 50 mM K-Epps buffer (pH 8.5), 20 mM $MgCl_2$, 0.1 mM EDTA, 5% (v/v) glycerol, 0.1% (w/v) gelatin, and 100 $\mu$Ci of [$\gamma$-$^{32}$P]ATP (6000 Ci/mmol; DuPont) diluted to a final concentration of 1 mM with cold ATP. KinA alone or in combination with Spo0F or Spo0A was included at the indicated concentrations. After incubation at 25 °C for the designated period of time, the reaction was terminated by the addition of 0.2 vol of stock 5-fold concentrated loading dye solution [250 mM Tris-Cl (pH 6.8)

[1] Abbreviations: IPTG, isopropylthiogalactoside; PMSF, phenylmethanesulfonylfluoride; Epps, 4-(2-hydroxyethyl)piperazine-1-propanesulfonic acid; Hepes, 4-(2-hydroxyethyl)piperazine-1-ethanesulfonic acid; Caps, 3-[cyclohexylamino]-1-propanesulfonic acid; Mes, 2-morpholinoethanesulfonic acid; Ampso, 3-(1,1-dimethyl-2-hydroxyethyl)amino-2-hydroxypropanesulfonic acid; Pipes, piperazine-1,4-bis-(2-ethanesulfonic acid); DTT, dithiothreitol; EDTA, ethylenediaminetetraacetic acid; NADH, $\beta$-nicotinamide adenine dinucleotide (reduced form), ADP, adenosine 5′-diphosphate; AMP-PCP, $\beta,\gamma$-methyleneadenosine 5′-triphosphate.

containing 10% (v/v) glycerol, 0.01% (w/v) bromphenol blue, 1% (w/v) SDS, and 280 mM 2-mercaptoethanol], and the sample was immediately frozen on dry ice until just prior to analysis by SDS−PAGE. Samples were loaded onto a 15% gel and electrophoresed at constant amperage (20 mA) for ~3 h, or until the dye front had migrated at least 75% of the gel length. The lower portion of the gel containing the dye front was removed to reduce background radiation due to unincorporated [$\gamma$-$^{32}$P]ATP (or contaminating [$\gamma$-$^{32}$P]$P_i$). The gel was dried at 80 °C under vacuum and exposed to Kodak X-OMAT AR film for 1 h at room temperature with two intensifying screens. Using the autoradiograph as a reference, the corresponding radioactive bands were excised and counted in water (Cerenkov radiation) using a Beckman LS 7500 scintillation counter. In addition, phosphorylated derivatives were detected and quantified on gels using a Molecular Dynamics phosphorimager.

For autophosphorylation of KinA, 1 $\mu$M final concentration of KinA was used and aliquots were withdrawn at various times for SDS−PAGE analysis to determine the time course for phosphate incorporation. For phosphotransfer to Spo0F, 0.1 $\mu$M KinA was routinely prelabeled for 5 min with ATP prior to starting the phosphotransfer reaction by final addition of Spo0F. For product (ADP) and dead-end (AMP-PCP) inhibition studies, the indicated concentration of inhibitor was included in the preincubation mixture. Analogous to the KinA autophosphorylation reaction, either individual reaction mixtures were quenched and analyzed at a given fixed time of reaction or, alternatively, aliquots were withdrawn from a large reaction mixture at various times and worked up as described above. KinA-mediated phosphotransfer to Spo0A was conducted in a similar manner except that the KinA concentration and the reaction times were normally increased at least 10-fold to ensure sufficient counts were incorporated into Spo0A-P, given the much lower turnover rate for Spo0A.

In one set of experiments, to determine the cause of substrate inhibition observed at high levels of Spo0F, the three reaction components (KinA, ATP, and Spo0F) were preincubated pairwise and the reaction started by the addition of the missing component. These assays were conducted and analyzed in all other respects in an identical manner to the normal fixed time point assay procedure. KinA-mediated phosphotransfer to Spo0F was also monitored continuously by coupling the rate of ATP hydrolysis to the pyruvate kinase and lactate dehydrogenase reactions, and measuring the rate of NADH disappearance fluorimetrically, essentially as described by Lowry and Passonneau (*24*). The standard assay contained (1.0 mL total volume) 50 mM K-Epps buffer (pH 8.5), 10 $\mu$M NADH, 0.4 mM phosphoenolpyruvate, 100 mM KCl, 20 mM $MgCl_2$, 1 mM DTT, 0.1 mM EDTA, 2 units of pyruvate kinase (rabbit muscle), and 10 units of lactate dehydrogenase (rabbit muscle). Coupling enzymes were added first to remove contaminating ADP and to allow determination of the KinA- or Spo0F-independent rate of NADH disappearance. Following addition of either KinA, Spo0F, or ATP to the preincubated reaction mixture containing the other two components, the rate was monitored continuously until complete conversion to Spo0F-P had occurred. The observed rate was corrected using appropriate blanks and the fluorescence scale was calibrated using known stock concentrations of NADH. Assays were monitored using a Perkin-Elmer model 650-40 fluorescence spectrophotometer equipped with a 150 W xenon lamp. Excitation and emission slits were set at 5 mm. Quartz cuvettes (1 mL, 1 cm path length) were used and all measurements were made at 25 °C. The excitation and emission wavelengths were 340 and 450 nm, respectively.

To determine the optimum pH for KinA-mediated reactions, including the overall phosphorelay from ATP to Spo0A-P via Spo0F-P and Spo0B-P, assays were performed as described above at roughly 0.5 pH intervals using the following series of buffers with overlapping pH ranges: Mes (pH 6.1 and 6.7), Pipes (pH 6.7 and 7.3), Hepes (pH 7.3 and 7.9), Epps (pH 7.9 and 8.5), Ampso (pH 8.5, 9.1, and 9.7), and Caps (pH 9.7 and 10.3). Assays were conducted over this pH range using a fixed concentration of substrates known to be saturating at pH 8.5; no attempt was made to insure saturation at the pH extremes. The "pH optima" described in the Results should thus be used only as a guide to the optimal assay conditions for each particular reaction and should not be construed as a true measure of the pH profile for either *V* or *V*/*K*.

*Complete Phosphorelay Pathway Assay*. For determination of the rate of Spo0A-P formation mediated by the entire phosphorelay, reactions were conducted in a manner similar to that described for Spo0F-P formation above, except that all components were present. To determine kinetic parameters for the two substrates (i.e., Spo0F-P and Spo0A) of the second putative phosphotransferase in this system, Spo0B, assay conditions were developed that would ensure a constant steady-state level of Spo0F-P. Thus, excess KinA (1 $\mu$M) was first preincubated with ATP (1 mM) for 5 min, and then with Spo0F (variable 1−10 $\mu$M) for 5 min. A limiting amount of Spo0B (0.05 $\mu$M) was then added, and finally Spo0A (variable 1−10 $\mu$M) was added to start the reaction. By using excess KinA (and ATP) and limiting Spo0B, we were able to maintain a constant Spo0F-P level equal to the initial Spo0F concentration throughout the linear portion of the Spo0A-P production time course.

*Data Processing*. Reciprocal initial velocities were plotted vs reciprocal substrate concentrations, and the experimental data were fitted by the least-squares method, assuming equal variance (constant absolute error) for the $v_i$ values (*25*), using the Fortran programs of Cleland (*26*). When the range of experimental velocities was a power of 10 or more, a constant proportional error was assumed and the $v_i$ values were fitted to the appropriate equation expressed in log form.

$$v_i = VA/(K_a + A) \quad (1)$$

$$v_i = VA/(K_a + A + A^2/K_I) \quad (2)$$

$$v_i = VAB/(K_{ia}K_b + AB + K_aB + K_bA) \quad (3)$$

$$v_i = VAB/(AB + K_aB + K_bA) \quad (4)$$

$$v_i = VA/(K_a(1 + I/K_{is}) + A) \quad (5)$$

$$v_i = VA/[K_a(1 + I/K_{is}) + A(1 + I/K_{ii})] \quad (6)$$

$$v_i = VA/[K_a + A(1 + A/K_{in})/(1 + A/K_{id})] \quad (7)$$

The points in the figures are the experimentally determined

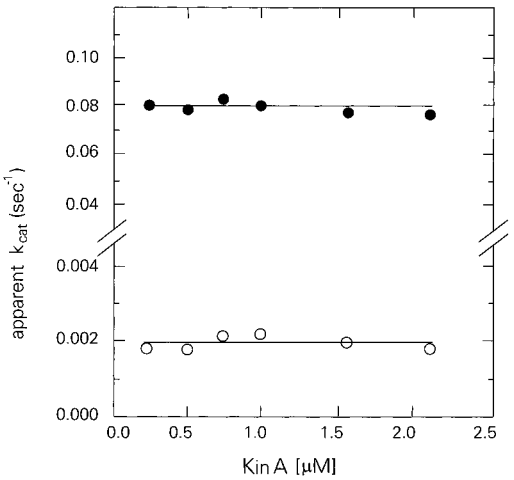


FIGURE 1: Enzyme concentration dependence for KinA-mediated reactions. The apparent $k_{cat}$ value (i.e., rate in micromolar per second/[KinA] in micromolarity) is constant for both KinA autophosphorylation (○) and KinA-mediated phosphotransfer to Spo0F (●). Rates were determined by fixed time point assay using standard reaction conditions (1.0 mM ATP with or without 10 $\mu$M Spo0F); the average apparent $k_{cat}$ values shown are: 0.0019 and 0.083 $s^{-1}$ for KinA autophosphorylation and for phosphotransfer to Spo0F, respectively.

values, and the curves are calculated from fits of the data to the appropriate equation. Linear double-reciprocal plots were fitted to eq 1; eq 2 was used when substrate inhibition was observed where $K_I$ is the substrate inhibition constant. Equation 3 describes an intersecting initial velocity pattern for a sequential bi-bi mechanism, where $v_i$ is the initial velocity, *A* and *B* are the substrate concentrations, $K_a$ and $K_b$ are the Michaelis constants for *A* and *B*, respectively, $K_{ia}$ is the dissociation for *A*, and *V* is the maximum velocity. Equation 4 describes a parallel initial velocity pattern for a ping-pong bi-bi mechanism, and is identical to eq 3 except for the missing constant term ($K_{ia}K_b$) in the denominator. In those cases where the enzyme concentration $[E]_{tot}$ was accurately known, we calculated values of $k_{cat} = V/[E]_{tot}$ (units of inverse seconds). Data conforming to linear competitive and linear noncompetitive inhibition were fitted to eqs 5 and 6, respectively, where *I* is the inhibitor concentration, and $K_{is}$ is the slope and $K_{ii}$ is the intercept inhibition constant. Equation 7 describes partial substrate inhibition by *A* where $K_{in}$ is the apparent inhibition constant and the limiting *V* is equal to $V(K_{in}/K_{id})$. The kinetic nomenclature used is that of Cleland (*27*).

## RESULTS

*KinA-Mediated Autophosphorylation and Spo0F-P Formation.* KinA mediates its own ATP-dependent autophosphorylation and the subsequent phosphotransfer to either Spo0F or Spo0A (*28*). Studies show a broad, bell-shaped dependence on pH for both KinA-mediated reactions, with the optimal rate occurring between pH 7.8 and 9.1 (data not shown). The "Good" buffer, Epps, was used at pH 8.5 in the present work as a prelude to definitive pH studies. Comparison of Tris-Cl and K-Epps buffers at pH 8.5 showed no significant difference in the rate or extent of reaction.

The rate of KinA autophosphorylation is independent of enzyme concentration over nearly a 10-fold range (Figure 1). Since many kinases, including KinA, are dimeric (*16*),

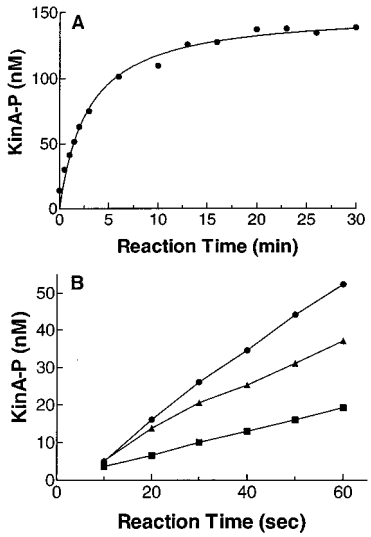


FIGURE 2: Time course of KinA autophosphorylation. KinA (0.5 $\mu$M) was incubated with 40 $\mu$M (■), 100 $\mu$M (▲), and 400 $\mu$M (●) ATP containing [$\gamma$-$^{32}$P]ATP in Epps buffer, pH 8.5, containing 20 mM $MgCl_2$ at 25 °C. Aliquots were removed from the reaction mixture and mixed with SDS−PAGE loading buffer at the time intervals indicated. Phosphorylated KinA was then separated and quantified by SDS−PAGE and phosphorimager analysis. Data shown represent results from three independent experiments. Diagram A is a full time course plot of the upper trace (400 $\mu$M ATP) illustrated as an initial rate in panel B.

Table 1: Kinetic Properties of KinA Autophosphorylation[a]

| | KinA autophosphorylation | |
|---|---|---|
| parameter | forward | reverse |
| $k_{cat}$ ($s^{-1}$) | 0.0019 ± 0.0005 | ND[b] |
| $K_m$ATP ($\mu$M) | 74 ± 11 | NA[c] |
| $K_m$ADP ($\mu$M) | NA | 16 ± 2.6 |

[a] Epps buffer (50 mM, pH 8.5), 1.0 $\mu$M KinA, variable ATP (50−250 $\mu$M), 25 °C, fixed time point assay. [b] ND, not determined. [c] NA, not applicable.

the phosphotransfer from the $\gamma$-phosphate of ATP to the putative active site His-403 residue of KinA probably proceeds by an interprotein reaction, as has been demonstrated in other similar systems (*17*). Autophosphorylation of KinA was carried out by incubating KinA with varying concentrations of ($\gamma^{32}$P) ATP and $Mg^{++}$, and the reaction was stopped at specified times by adding SDS−PAGE loading buffer. Phosphorylated KinA (KinA-P) was separated from excess ATP by SDS−PAGE and was quantified with the phosphorimager. Autophosphorylation was linear with time in the first minute of reaction (Figure 2B) at 40, 100, and 400 $\mu$M ATP and showed a saturable time course over a period of 30 min (Figure 2A). The $k_{cat}$ and $K_m$ for ATP measured within the linear phase of the reaction were 0.0019 $s^{-1}$ and 74 $\mu$M, respectively (Table 1). ADP inhibited KinA autophosphorylation in competition with ATP with a $K_i$ value of 43 $\mu$M. KinA autophosphorylation displayed an absolute requirement for divalent metal ions, the reaction rate dropping significantly in the presence of 2 mM EDTA. The concentration dependence was such that $Mg^{++}$ ions stoichiometric with ATP produced full activity, while levels higher gave inhibition ($K_i \cong 20$ mM).

KinA-P underwent dephosphorylation in the presence of ADP. In the absence of ADP, KinA-P was relatively stable under the experimental conditions (see Materials and Meth-

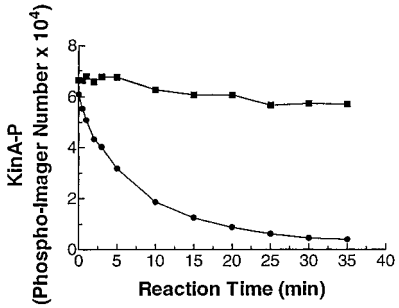


FIGURE 3: Dephosphorylation of phosphorylated KinA in the presence and absence of ADP. Purified phosphorylated KinA (0.13 $\mu$M, approximately 2900 cpm/pmol) was incubated with (●) or without (■) 200 $\mu$M ADP at 25 °C. At the indicated time interval, aliquots were removed from the reaction mixture and mixed with SDS−PAGE loading buffer. Phosphorylated KinA was then separated and quantified by SDS−PAGE and Phosphorimager analysis. Data shown represent results from three independent experiments.

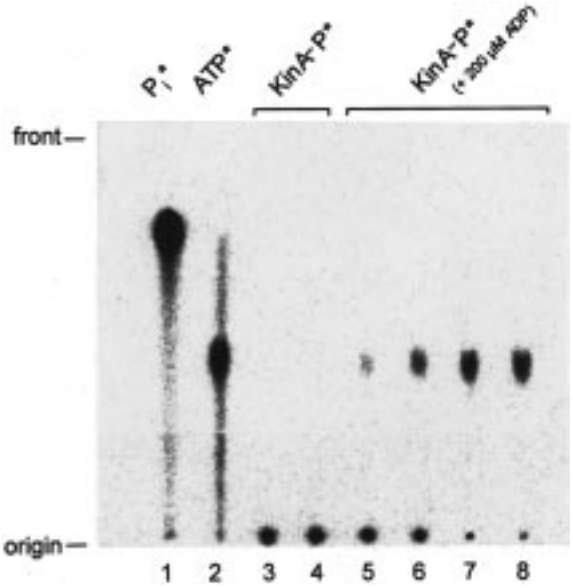


FIGURE 4: Product of dephosphorylation by ADP of phosphorylated KinA (KinA-P). Purified KinA-P (0.13 $\mu$M, approximately 2900 cpm/pmol) was incubated with or without 200 $\mu$M ADP at 25 °C. At various intervals, aliquots were removed from the reaction mixture and spotted onto a PEI-cellulose TLC plate. The TLC plate was then developed with 1.2 M LiCl and analyzed by the phosphorimager. Lane 1, [$^{32}$P]phosphate; lane 2, [$\gamma$-$^{32}$P]ATP; lanes 3 and 4, KinA-P, incubated for 0 and 30 min at 25 °C, respectively; lanes 5 to 8, KinA-P incubated with 200 $\mu$M ADP at 25 °C for 0.5, 1, 10, and 30 min, respectively. P* corresponds to [$^{32}$P]phosphate.

ods) (Figure 3). To determine the product of this dephosphorylation reaction, KinA-P was incubated with ADP and the reaction was analyzed by TLC. As shown in Figure 4, the product of the dephosphorylation was ATP, no free phosphate was generated. The ADP-dependent dephosphorylation of KinA-P showed a saturable time course with a linear phase within the first minute of the reaction at 20, 100, and 200 $\mu$M ADP (data not shown). The $K_m$ for ADP in the dephosphorylation reaction, measured within the linear period of the reaction, was 16 $\mu$M (Table 1).

The rate of KinA-mediated phosphotransfer to Spo0F (Figure 1) or Spo0A (data not shown) was also independent of enzyme concentration although the rate was enhanced relative to that observed for KinA autophosphorylation

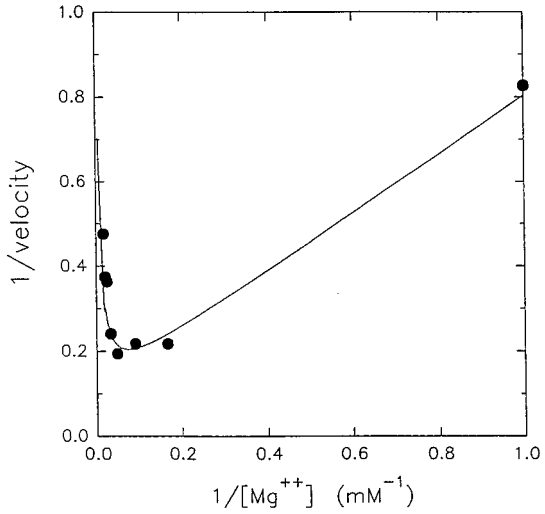


FIGURE 5: Magnesium ion concentration dependence for Spo0F-P formation. Double-reciprocal plot showing both activation ($k_{act}$ = 7.5 ± 1.5 mM) and inhibition ($K_i$ = 24 ± 3 mM) by $Mg^{++}$ for KinA-mediated phosphotransfer to Spo0F. Points show experimental rates determined by the fixed time point assay using standard reaction conditions (1.0 mM ATP, 0.1 $\mu$M KinA, and 10 $\mu$M Spo0F) and the indicated concentration of $MgCl_2$; the line is a fit to eq 7.

(Figure 1). As shown in Figure 5, KinA-mediated Spo0F-P formation also displayed both activation and inhibition by $Mg^{++}$. $K_{act} \cong 7$ mM was much higher, however, suggesting another site for the metal ion in addition to the Mg−ATP chelate complex required for autophosphorylation. The inhibition shown in Figure 5 appears to be partial, rather than complete, with an apparent $K_i$ = 24 mM. Monovalent cations (e.g., $Na^+$ and $K^+$) neither stimulated nor inhibited either reaction. KinA-mediated Spo0F-P formation showed substrate inhibition by high levels of Spo0F, but only when the latter was preincubated with KinA in the absence of ATP (Figure 6). The fact that prior reaction of KinA with ATP prevented substrate inhibition suggested that an abortive KinA·Spo0F complex could form, but only with the unphosphorylated kinase. Substrate inhibition by Spo0F was total, rather than partial, and was noncompetitive versus ATP with $K_{ii} \cong K_{is} \cong 10$ $\mu$M (data not shown). The low affinity of Spo0F for $Mg^{++}$ ($K_d \approx 20$ mM) measured by both fluorimetric and NMR techniques (*29*) confirms that the reduced rate of phosphorylation at higher concentrations of Spo0F cannot be associated with depletion of the divalent cation, but is most probably caused by a genuine protein−protein interaction. Regardless of the assay method employed to monitor Spo0F-P formation (i.e., either the standard fixed time point assay using [$\gamma$-$^{32}$P]ATP or the continuous fluorimetric assay), a transient increase was routinely observed from an initially slow rate to a final steady-state rate that was roughly 4-fold faster when Spo0F was added last to initiate the reaction (Figure 7A). This transient did not occur upon addition of a second aliquot of either KinA or Spo0F to the assay mixture, confirming that the effect did not arise from a single hysteretic transition caused by adding either protein to the assay mixture (*30*). Transition to the faster rate was complete when the Spo0F-P produced was roughly equivalent to the concentration of KinA present in the assay.

*Lag Phase in the Time Course of KinA-Mediated Phosphorylation of Spo0F*. To understand this lag phase, KinA-

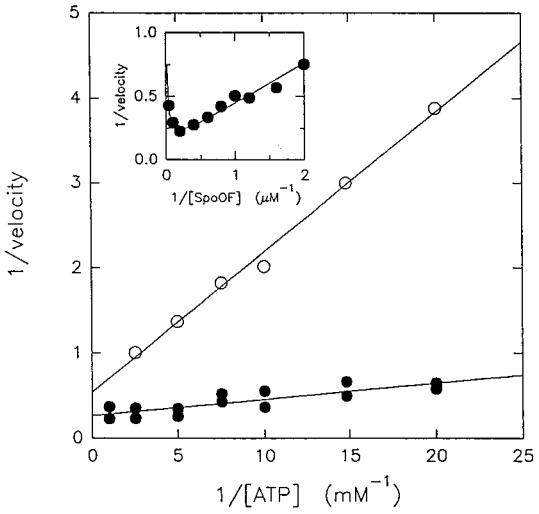


FIGURE 6: Substrate inhibition by Spo0F depends on the order of addition. A double reciprocal plot showing a 2.5-fold and 7.5-fold decrease, respectively, in apparent $K_m$ and $V/K$ for ATP at 100 $\mu$M Spo0F concentration when ATP was added last (○) compared to when either KinA or Spo0F was added last (●) to start the Spo0F-P formation reaction. Rates were determined by fixed time point assay using standard reaction conditions (1 $\mu$M KinA, 100 $\mu$M Spo0F) after a 5 min preincubation of any two of the three reaction components. The inset double-reciprocal plot shows substrate inhibition by Spo0F (1.0 mM ATP and 0.1 $\mu$M KinA) with $K_m$ = 2.8 ± 0.8 $\mu$M and $K_i$ = 9.3 ± 3.2 $\mu$M.

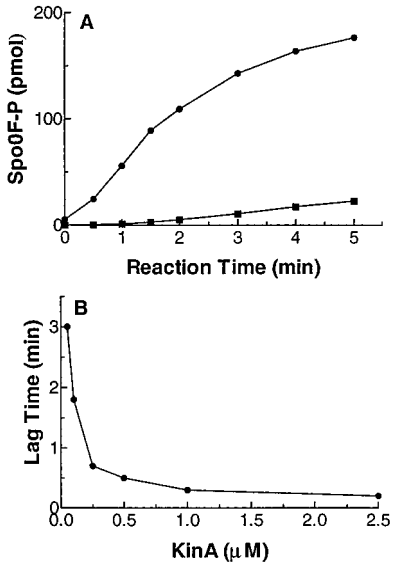


FIGURE 7: (A) Lag phase in the time course of KinA-mediated Spo0F phosphorylation. Phosphorylation reactions were carried out with 0.1 $\mu$M KinA (■) and 0.5 $\mu$M KinA (●), 10 $\mu$M Spo0F, and 400 $\mu$M ATP containing [$\gamma$-$^{32}$P]ATP in Epps buffer, pH 8.5 containing 20 mM $MgCl_2$ at 25 °C. The reactions were initiated by addition of KinA. Aliquots were removed from the reaction mixture and mixed with SDS−PAGE loading buffer at the time intervals indicated. Phosphorylated Spo0F was then separated and quantified by SDS−PAGE and phosphorimager analysis. Data shown represent results from three independent experiments. (B) Effect of KinA concentration on the lag phase of KinA mediated Spo0F phosphorylation. Phosphorylation reactions were carried out with various concentrations of KinA as indicated, 5 $\mu$M Spo0F, and 100 $\mu$M ATP containing [$\gamma$-$^{32}$P]ATP in Epps buffer, pH 8.5, containing 20 mM $MgCl_2$ at 25 °C. The reactions were initiated by addition of KinA. Aliquots were removed from the reaction mixture and mixed with SDS−PAGE loading buffer at 0.25, 0.5, 1, 2, 4, 6, 8, 10, and 15 min after addition of KinA. Phosphorylated Spo0F was then separated by SDS−PAGE and quantified by scintillation counting of the bands excised from the gel. Lag time was defined as the time point where a linear phase started.

mediated Spo0F phosphorylation was carried out under various conditions, and the time courses of Spo0F phosphorylation were examined and compared. When the concentrations of ATP and Spo0F were kept constant, the length of time of the lag phase was dependent on KinA concentration with a longer lag phase at low KinA concentration and shorter lag phase at high KinA concentration (Figure 7B). At 0.5 $\mu$M KinA, the lag time was about 0.5 min. This KinA concentration was used in experiments measuring kinetic parameters of KinA-mediated Spo0F phosphorylation, since this lag time could even be shortened to a negligible level under certain conditions. Thus, preincubation of KinA with [$\gamma$-$^{32}$P]ATP for 3 min prior to addition of Spo0F shortened the lag time to an extent that it was negligible at both 40 and 400 $\mu$M ATP. Neither ATP nor Spo0F affected the lag phase in a concentration dependent manner (data not shown). The length of time of the lag phase was also affected by temperature. The lag time was significantly shorter when the reaction was carried out at 30 °C compared with that at 25 °C.

In practical terms, if the kinetic transient or lag phase was ignored, the results from single fixed time point assays at each pair of substrate concentrations yielded a nonlinear double-reciprocal plot of $1/v_i$ versus 1/[ATP], since at the lower ATP concentrations the reaction never reached the "fast" phase. However, by employing a high initial [Spo0F]/[KinA] ratio (e.g., ≥ 15) and running the reaction to a constant percentage of Spo0F turnover (e.g., Δ[Spo0F]/$[Spo0F]_{tot}$ ≅ 20%), we were able to show that at a fixed Spo0F concentration the lag time as a function of ATP concentration comprised a constant fraction of the overall reaction time course, and could thus be ignored. For experiments where the Spo0F concentration was varied at a fixed level of ATP (i.e., dead-end and product inhibition studies versus Spo0F), using this method resulted in a slight underestimation of the rates at low [Spo0F] due to the relatively larger proportional contribution of the lag time to the overall time course. Comparison of data from single time point assays with those obtained from complete time course analyses, however, showed that this error was within the noise of the experimental method.

*Initial Velocity Studies*. Figure 8 shows an initial velocity pattern determined using a matrix of Spo0F and ATP concentrations for the reaction ATP + Spo0F ⟹ ADP + Spo0F-P. Because the resulting pattern appeared to be almost parallel, the entire data set was fitted to the equations describing a sequential (eq 3) and a ping-pong (eq 4) kinetic mechanism. Table 2 lists the kinetic parameters obtained. Ignoring the constant $K_{ia}K_b$ term (eq 4) actually lowers the SIGMA value (square root of the residual least squares) from 0.119 to 0.115, suggesting that this term is not statistically significant. Not surprisingly, therefore, $K_{ia}$ (ATP) was not well determined by the data (i.e., the standard error for $K_{ia}$ is greater than the fitted value), since in a sequential mechanism $K_{ia}$ must be substantially less than the $K_m$ for ATP in order to produce the nearly parallel initial velocity pattern shown in Figure 8.

The results for KinA-mediated phosphotransfer to Spo0A were also consistent with a low value for $K_{iATP}$. Thus, because direct phosphotransfer to Spo0A is very slow relative

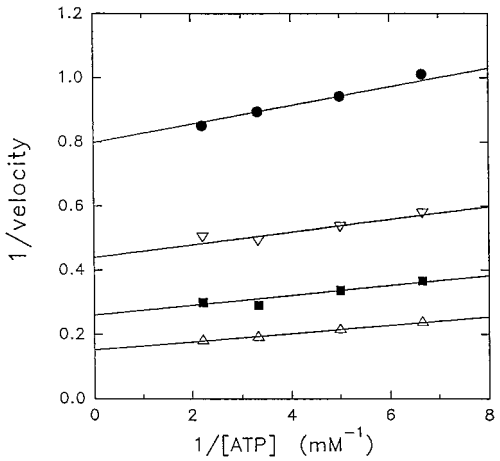


FIGURE 8: Initial velocity pattern for KinA-mediated Spo0F-P formation. Representative double-reciprocal plot of $1/v_i$ versus 1/[ATP] at various Spo0F concentrations: 1.53 $\mu$M (●) , 2.5 $\mu$M (▽), 4.0 $\mu$M (■), and 10.0 $\mu$M (△). Rates determined from time-courses of [$^{32}$P]Spo0F-P production under standard conditions (0.1 $\mu$M KinA) were calculated for the reaction occurring after the lag phase. The lines are calculated from a fit to eq 3.

Table 2: Comparison of Kinetic Parameters for KinA-Mediated Reactions

| | phosphotransfer to Spo0F[a] | | |
|---|---|---|---|
| parameter | sequential | ping-pong | phosphotransfer to Spo0A[b] |
| $K_{Spo0X}$ ($\mu$M) | 2.1 ± 0.3 | 2.1 ± 0.2 | 23 ± 10 |
| $K_{ATP}$ ($\mu$M) | 77 ± 11 | 80 ± 7 | ∼0 |
| $K_{iATP}$ ($\mu$M) | 4 ± 13 | | |
| $k_{cat}$ ($s^{-1}$) | 0.083 ± 0.005 | 0.085 ± 0.004 | $1.5 \times 10^{-5}$ |
| $k_{cat}/K_{Spo0X}$ ($M^{-1}$ $s^{-1}$) | 39 000 | 40 000 | 0.7 |
| SIGMA | 0.119 | 0.115 | |

[a] Epps buffer (50 mM, pH 8.5), 0.1 $\mu$M KinA, variable ATP (50−250 $\mu$M), variable Spo0F (1.5−10 $\mu$M), 25 °C, full time-course analysis using [$^{32}$P]ATP. [b] Epps buffer (50 mM, pH 8.5), 0.1 $\mu$M KinA, variable Spo0A (5−50 $\mu$M), 0.1 mM ATP, 25 °C, fixed time point assay.

to either KinA autophosphorylation or phosphotransfer to Spo0F (cf. Table 2), the reaction of KinA with ATP to generate E-P should be at equilibrium during Spo0A turnover. As such, the relevant kinetic parameter for ATP will be the equilibrium dissociation constant, $K_{ia}$, rather than the Michaelis constant, $K_a$. Because we saw no variation in the rate of Spo0A-P formation for [ATP] = 20−100 $\mu$M when a nonsaturating level of Spo0A (10 $\mu$M) was used, the data imply that $K_{ia} \leq 2$ $\mu$M. Comparison of the kinetic parameters for KinA-mediated Spo0F-P and Spo0A-P formation (Table 2) shows that, in catalytic efficiency terms ($k_{cat}/K_{SpoOX}$), Spo0F is a 57000-fold better substrate for KinA than is Spo0A!

*Product and Dead-End Inhibition Studies*. The product, ADP, and the nonhydrolyzable ATP analog, AMP-PCP, were linear competitive inhibitors against ATP in both the KinA autophosphorylation and the KinA-mediated Spo0F-P formation reactions. When tested against Spo0F in the latter reaction, both compounds were linear noncompetitive inhibitors. Table 3 lists the inhibition constants obtained by least-squares analysis of the data using eqs 5 and 6. As shown, ADP was the more potent inhibitor with $K_i$ values at least 30-fold lower than for AMP-PCP. Apparent $K_i$ values for both compounds as inhibitors against Spo0F increased linearly with increasing ATP concentration (data not shown), consistent with inhibition arising solely from competition with ATP at the active site. These results are consistent with an ordered sequential kinetic mechanism for the phosphotransfer reaction in which ATP adds before Spo0F and ADP is the last product to leave.

*Kinetic Parameters for Spo0B-Mediated Reactions*. By using excess KinA and ATP to maintain a constant steady-state level of Spo0F-P during turnover of Spo0A to Spo0A-P via the complete phosphorelay, we were able to determine the kinetic parameters for the two "substrates" of the Spo0B-mediated reaction, namely Spo0F-P and Spo0A. Inspection of a representative experimental time course (Figure 9) confirms that steady-state levels of KinA-P, Spo0F-P, and Spo0B-P are achieved rapidly and are maintained throughout the linear region of Spo0A-P production. The results of fits to eq 1 of reaction rate data derived from similar time courses are listed in Table 4. Of particular note is the fact that the catalytic efficiency for phosphotransfer from Spo0B-P to Spo0A is 20-fold and 1.1-million-fold *greater* than that for direct phosphotransfer from KinA-P to Spo0F and Spo0A, respectively. The rate of Spo0A-P formation via the complete phosphorelay displayed a linear dependence on the Spo0B concentration (Figure 9). The pH optimum for the complete phosphorelay assayed under conditions where the Spo0B-mediated reaction was rate determining was found to be shifted to lower pH relative to either of the other KinA-mediated reactions, with an optimum near pH 7.5 (data not shown).

## DISCUSSION

Approaching 100 histidine protein kinase/phosphoaspartate response regulator systems have now been described in the biochemical literature (*1*), but few are known to involve the direct transfer of the $\gamma$-phosphate of ATP via *four* distinct proteins as occurs with the phosphorelay system controlling sporulation in *B. subtilis*. Our initial suggestion as to why nature would invoke such a complex scheme in this particular case was one of enhanced control. Thus, in order to make the crucial decision whether to pursue vegetative growth or spore formation, the bacterium must be able to integrate a variety of environmental factors and translate this information into the expression of specific genes. Having the two extra components in the phosphorelay, plus additional recently discovered phosphatase regulatory proteins (*8*), in principle, provides the opportunity for enhanced control of bacterial sporulation. As described in this report, the four component phosphorelay pathway displays some unique synergistic kinetic effects derived from interactions between the various components, which may prove to be the means by which this system is modulated by environmental stimuli.

First, consider the autophosphorylation of KinA. By analogy with CheA and several other kinases (*16*), KinA is dimeric and probably transfers the $\gamma$-phosphate of bound ATP intermolecularly to its dimeric counterpart, presumably to His-403 (*17*). In this regard, KinA is different from several serine and threonine protein kinases where autophosphorylation has been shown to occur via an intrapeptide reaction (*31*−*33*). In those cases, however, autophosphorylation merely serves to activate or otherwise modulate the activity of the kinase toward exogenous protein substrates.

Table 3: Product and Dead-End Inhibition Studies of KinA-Mediated Reactions

| | | ADP | | AMP-PCP |
|---|---|---|---|---|
| KinA autophosphorylation versus ATP[a] | C[d] | $K_{is} = 45 \pm 6\ \mu M$ | C | $K_{is} = 1.1 \pm 0.3$ mM |
| phosphotransfer to Spo0F versus ATP[b] | C | $K_{is} = 46 \pm 8\ \mu M$ | C | $K_{is} = 1.3 \pm 0.4$ mM |
| versus Spo0F[c] | NC | $K_{is} = 52 \pm 15\ \mu M$ | NC | $K_{is} = 3.5 \pm 1.0$ mM |
| | | $K_{ii} = 95 \pm 2\ \mu M$ | | $K_{ii} = 1.5 \pm 0.1$ mM |

[a] Epps buffer (50 mM, pH 8.5), 1.0 $\mu$M KinA, variable ATP (50−250 $\mu$M), 25 °C, fixed time point assay. [b] Epps buffer (50 mM, pH 8.5), 1.0 $\mu$M KinA, variable ATP (50−250 $\mu$M), 10 $\mu$M Spo0F, 25 °C, fixed time point assay. [c] Epps buffer (50 mM, pH 8.5), 1.0 $\mu$M KinA, variable Spo0F (1−10 $\mu$M), 0.1 mM ATP, 25 °C, fixed time point assay. [d] C = competitive, NC = noncompetitive.

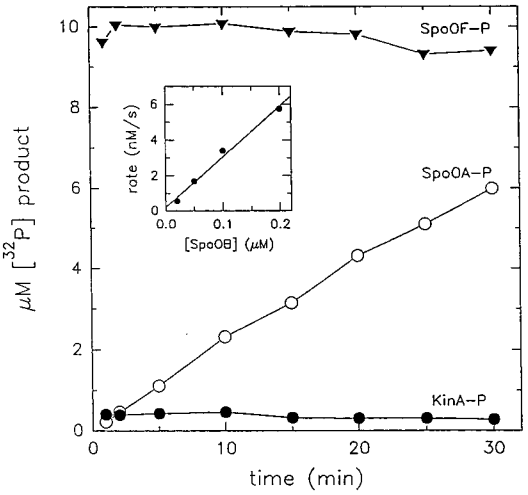


FIGURE 9: Time course for Spo0B-mediated Spo0A-P formation using the Spo0F-P regeneration system. Reaction was started by the addition of Spo0B following 5 min preincubation of KinA with Spo0F and ATP to preform Spo0F-P. The constant rate of Spo0A-P production over 30 min corresponds to a calculated $k_{cat} = 0.094$ $s^{-1}$ for Spo0B catalysis. Spo0F-P (▼), KinA-P (●), and Spo0A-P (○) levels were determined by fixed time point assay using standard conditions with 1.0 mM ATP, 0.5 $\mu$M KinA, 10 $\mu$M Spo0F, 10 $\mu$M Spo0A, and 0.1 $\mu$M Spo0B. Inset shows a linear dependence of the rate of Spo0A-P production on Spo0B concentration.

Table 4: Kinetic Parameters for the Spo0B-Mediated Reaction

| parameter | complete phosphorelay system[a] |
|---|---|
| $K_{Spo0F-P}$ ($\mu$M) | $20 \pm 4$ |
| $K_{Spo0A}$ ($\mu$M) | $0.25 \pm 0.10$ |
| $k_{cat}$ (s-1) | $0.20 \pm 0.04$ |
| $k_{cat}/K_{SPo0F-P}$ ($M^{-1}$ $s^{-1}$) | 10 000 |
| $k_{cat}/K_{Spo0A}$ ($M^{-1}$ $s^{-1}$) | 800 000 |

[a] Epps buffer (50 mM), 0.05 $\mu$M Spo0B, 1.0 $\mu$M KinA, variable Spo0A (0.5−5 $\mu$M) at 10 $\mu$M fixed Spo0F-P (generated *in situ*), variable Spo0F-P (1−10 $\mu$M generated *in situ*) at 10 $\mu$M fixed Spo0A, 25 °C, time-course analysis to determine initial rates.

In the phosphorelay, as in the simpler two-component systems (*1*), the phosphoenzyme is actually an intermediate in the subsequent phosphotransfer reaction(s). The fact that autophosphorylation is an internal reaction implies flexibility in the KinA structure to allow interaction between the putative nucleotide binding region,[2] and the domain containing His-403. Unlike many of the histidine protein kinases described to date (*1*), the KinA sequence does not contain any recognizable membrane-spanning regions (*33*). Kinetic results reported for autophosphorylation of additional soluble histidine protein kinases, namely CheA (*16*), EnvZ (*34*), and NtrB (*35*), also support a dimeric reaction mechanism. It remains to be established whether this is a general property of all the systems.

KinA autophosphorylation and KinA-mediated phosphotransfer to Spo0F each require $M^{++}$ ions (Figure 5). As with most ATP-utilizing kinases, one equivalent of $M^{++}$ present as an $M^{++}$−ATP chelate complex is likely to serve as the actual substrate for the autophosphorylation reaction (*36*). However, because the $K_d$ value for Mg−ATP formation at pH 8.5 [0.013 mM (*36*)] is nearly 500-fold lower than the apparent $K_{act} = 7$ mM (Figure 5), the data suggest a second role for $M^{++}$ in KinA-mediated phosphotransfer to Spo0F (and Spo0A). Using a similar two component system, others have shown that in order for effective phosphotransfer to occur from the phosphorylated kinase (CheA-P), the response regulator (CheY) must first contain bound $M^{++}$ (*37*). CheA-mediated dephosphorylation of CheY-P also requires a divalent metal ion.

Given the known chemistry of these two component systems (*1*, *38*), one would predict that KinA-mediated Spo0F-P formation should follow a classical ping-pong bi-bi kinetic mechanism where a piece of the first substrate (ATP) is transferred to the enzyme (KinA) and the first product (ADP) leaves *before* the second substrate (Spo0F) binds and reacts. A ping-pong mechanism is supported by the fact that both half-reactions can be observed in the absence of the other substrate. Specifically, the phosphoryl group of KinA-P can be transferred directly to both ADP (Figure 4) and Spo0F (Figure 10). In that case, the first half-reaction should necessarily be unaffected by the presence of the second substrate, and hence one should see a parallel initial velocity pattern (*27*). The initial velocity pattern shown in Figure 8 indeed appears to be nearly parallel. Analysis reveals, however, that the data are in fact almost equally well described by the equation for a sequential kinetic mechanism (eq 3), and that the nearly parallel pattern could simply be due to the fact that $K_{ia} << K_a$, where A, the first substrate, is ATP.

Support for this conclusion comes from the observation of pronounced substrate synergism by Spo0F of the rate of KinA autophosphorylation. Thus, under optimal conditions $k_{cat}$ for KinA, autophosphorylation is ~0.0019 $s^{-1}$, while when Spo0F is present $k_{cat}$ for the same reaction increases up to 40-fold (Tables 1 and 2, Figure 1). The fact that Spo0F *enhances* the rate of KinA autophosphorylation suggests that Spo0F is bound to KinA during the reaction. Yet, the observation of substrate inhibition by Spo0F at high concentration (cf. Figure 6) implies that formation of a distinct E·Spo0F complex can also occur and lead to inhibition.

[2] The glycine rich sequence (GTGLGL) beginning at residue 569 in KinA is highly conserved among prokaryotic histidine protein kinases (*1*) and resembles various nucleotide binding motifs identified in other ATP- and GTP-dependent enzymes (*2*−*4*).

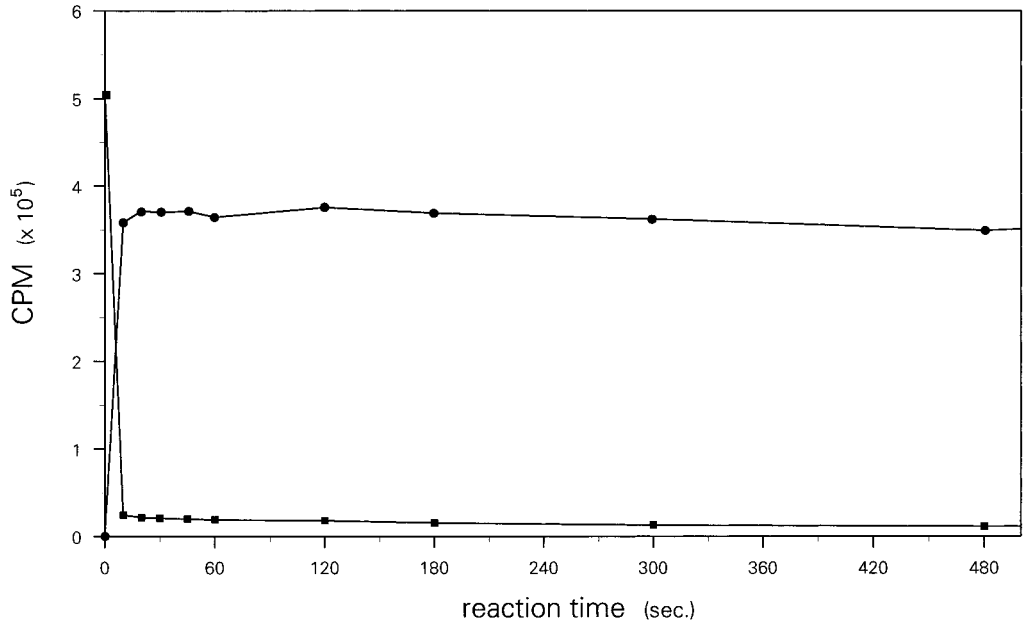


FIGURE 10: [$\gamma^{32}$P]-Labeled KinA-P (~0.1 $\mu$M), purified by Superose-12 FPLC column chromatography, was incubated with aliquots of Spo0F (10 $\mu$M) in the standard reaction buffer solution (Materials and Methods). At each time point, the reaction was terminated with the usual concentrated loading dye solution followed by SDS−PAGE separation and phosphorimager analysis. Transfer of radioactivity associated with phosphoryl transfer from KinA-P (■) to Spo0F (●) is plotted with time.

Scheme 1 outlines the proposed overall reaction sequence that could accommodate these observations:

Scheme 1

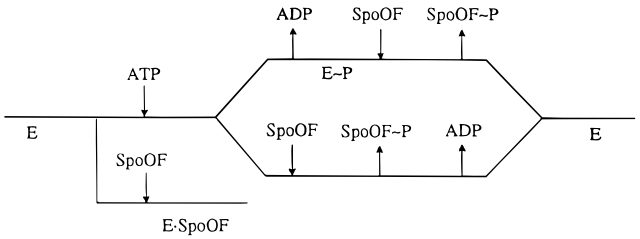


Scheme 1 consists of two branches: (1) the upper branch represents a classical ping-pong bi-bi reaction in which ATP binds to the enzyme first, then reacts to form the phosphohistidine moiety on KinA, followed by release of ADP prior to Spo0F binding, transfer of the phosphoryl group to the aspartate receptor of Spo0F, and finally release of Spo0F-P; and (2) the lower branch corresponds to a sequential bi-bi mechanism in which Spo0F binds *prior* to the release of ADP. The order of product release is based on the observation that ADP is a competitive product inhibitor against ATP ($K_{is} \cong 45$ $\mu$M) in both the autophosphorylation and Spo0F-P formation reactions, consistent with both nucleotides binding to free enzyme. To explain the experimental results, the rate-controlling step for the first half-reaction (up to and including the release of ADP) along the upper branch must be facilitated by Spo0F such that when Spo0F is present reaction proceeds predominantly along the lower branch. Additionally, as noted above, Spo0F can interact directly with enzyme to form an inactive complex, although this avenue is only weakly pursued as high concentrations of Spo0F are required to exhibit inhibition.

The initial lag phase in the formation of Spo0F~P (Figure 7) could occur for several reasons. For example, it could reflect the time required for the first round of KinA autophosphorylation, since the rate of KinA autophosphorylation is slower than the rate of KinA mediated Spo0F phosphorylation (Figure 1). Or it is possible the lag phase reflects the time required for a conformational change or alignment of the dimeric kinase induced by interaction of KinA with ATP, or KinA with Spo0F or Spo0F with ATP, or it could be a combination of each of these possibilities.

To address the various possibilities, preincubation was carried out under various conditions and the effect on the lag time was examined. Preincubating KinA with low concentrations of nonradioactive ATP (1 $\mu$M) for 3 min followed by addition of Spo0F and 400 $\mu$M [$\gamma$-$^{32}$P]ATP had no effect on the lag phase. Similarly, preincubating KinA with ADP at low concentrations (1 and 20 $\mu$M) followed by addition of Spo0F and 400 $\mu$M [$\gamma$-$^{32}$P]ATP had no effect on the lag phase, while at high ADP concentration (200 $\mu$M), inhibition of Spo0F phosphorylation occurred. Preincubating KinA with Spo0F for 5 min prior to addition of [$\gamma$-$^{32}$P]ATP had no effect on the lag phase at both 0.1 and 0.5 $\mu$M KinA. Preincubation of Spo0F with ATP had no effect on the lag phase either. The results suggested that the lag phase was not related to a conformational change induced by interaction of KinA with ATP or ADP, KinA with Spo0F, or Spo0F with ATP.

The lag phase was reduced considerably when the ATP concentration in the preincubation mix was the same as that of the overall reaction. Thus, when KinA was preincubated with 400 $\mu$M nonradioactive ATP for 3 min followed by addition of Spo0F and an equal concentration of [$\gamma$-$^{32}$P]ATP, the lag was shortened to a negligible level. However, when KinA was preincubated with 20 $\mu$M nonradioactive ATP for 3 min, followed by addition of Spo0F and 400 $\mu$M of [$\gamma$-$^{32}$P]-ATP, no significant lowering of the lag time was observed, compared to no preincubation. This result suggests that not only formation of KinA-P, but also the relative concentration

of KinA-P in the preincubation mix compared to that in the final reaction affects the lag time.

An alternative possibility that activation of KinA by initial phosphoryl transfer from ATP to histidine is a prelude to direct phosphoryl transfer from subsequently bound ATP molecules to Spo0F is unlikely as the experimental results included in Figure 10 show that KinA-P purified from nucleotide phosphate is a ready donor of its phosphoryl group to Spo0F. Nevertheless, there is the possibility that the initial phosphoryl group from bound ATP could transfer to its complementary histidine and cause the second molecule in the dimeric kinase to be placed in a more active state so that it then could more readily accommodate and transfer the phosphoryl group. This interesting hypothesis remains to be explored.

Substrate synergism could arise if Spo0F binding to E·ATP enhanced the rate of either KinA-P formation or of ADP release from E-P·ADP. Why is substrate inhibition by Spo0F not observed (at least over the same Spo0F concentration range) when KinA is preincubated with ATP? The answer may lie in the relative binding affinities of ATP and Spo0F, since during turnover both will compete for the free enzyme. Initial velocity data for both Spo0F-P and Spo0A-P formation indicate that $K_{ia}$ for ATP is $\leq 2$ $\mu$M, while the $K_I$ value for Spo0F inhibition is near 10 $\mu$M. Alternatively, after the first turnover, Spo0F-P may prevent formation of the abortive E·Spo0F complex by blocking the putative activator/inhibitor site.

There is good precedent for hybrid ping-pong/sequential mechanisms. Elegant studies of *Escherichia coli* succinyl coenzyme A synthetase, an enzyme that forms a covalent E:His-P intermediate en route to formation of an acylphosphate mixed anhydride at the enzyme active site analogous to the KinA-P and Spo0F-P intermediates of the phosphorelay system, have demonstrated pronounced substrate synergism leading to an intersecting initial velocity pattern for what is in reality a ping-pong type chemical mechanism (*39*, *40*). In that case, the initial rate of E-P formation in the presence of the alternate substrates was found to be much faster than either the rate of net product formation or the rate of E-P formation in the absence of substrate-induced synergism, as occur with KinA.

This pattern of substrate activation *in vitro* has interesting parallels in the cellular concentration of the two components *in vivo*. Transcription of the *Spo0F* gene is tightly controlled by environmental factors, whereas *kinA* transcription is virtually constitutive. Under good growth conditions where the cellular Spo0F concentration is very low, the autophosphorylation activity of the kinase is thus inactive. This prevents, among other things, phosphate transfer to heterologous response regulators and spurious activation of nonrelated signal transduction pathways. The elevated level of cellular Spo0F resulting from increased *Spo0F* transcription during the initiation of sporulation may serve to activate KinA and, thus, the overall phosphorelay pathway (*39*).

Conformational changes have been postulated to occur upon phosphorylation of the various response regulators, based on the observation that binding to their respective DNA control elements is greatly enhanced following phosphorylation (*30*). In addition, mutants of both CheY (*41*) and OmpR (*42*) have been isolated that will function without being phosphorylated, suggesting that a single point mutation alone can induce the active conformation.

Perhaps more striking is the ability of KinA to discriminate so effectively between Spo0F and Spo0A. As noted in Table 2 the $k_{cat}/K_{SpoOX}$ value for KinA-mediated Spo0F-P formation is 57000-fold greater than that for Spo0A-P formation. This occurs despite the fact that Spo0F and Spo0A are known to have similar N-terminal sequences surrounding the tri-aspartate pocket that undergoes phosphorylation (*43*, *44*). These kinetic properties are, furthermore, consistent with the genetics of the phosphorelay. Strains with mutations in the *Spo0F* or *Spo0B* genes are unable to produce even low amounts of Spo0A-P indicating that KinA does not phosphorylate Spo0A directly *in vivo*. Single missense point mutations in Spo0A, *sof* mutations, make the altered Spo0A an effective substrate for KinA (*45*). Both *sof* mutations in Spo0F and raising the cellular level of Spo0A by genetic means can bypass the phosphorelay in a KinA-dependent manner. The ability to kinetically characterize these protein substrates for KinA offers a unique opportunity to discern exactly what are the structural determinants in Spo0F that contribute to effective binding and catalysis by KinA.

Quantitatively speaking, the largest discrimination is seen when one compares Spo0A as a substrate for phosphorylation by either KinA or Spo0B. As one can calculate from the values in Tables 2 and 4, $k_{cat}/K_{Spo0A}$ for Spo0B catalysis is 1.1-*million*-fold greater than that for the KinA-mediated reaction. Spo0B is the most unique protein component of the sporulation phosphorelay, with no obvious homology to any known "kinase" and with the ability to catalyze efficient phosphate transfer between itself and *both* Spo0F and Spo0A without any dependence on ATP. As such, it is not surprising that Spo0B should show kinetic properties that are distinct from all of the other histidine protein kinases identified to date. In addition, having developed a system for maintaining a constant steady-state level of Spo0F-P (via KinA/ATP recycling), we are now in a position to kinetically characterize the various *sof* mutants of Spo0A to determine precisely how these mutant proteins manage to circumvent the lack of Spo0F in the cell.

## ACKNOWLEDGMENT

The authors are indebted to Tom Bray for technical support and James Zapf for helpful discussions.

## REFERENCES

1. Stock, J. B., Surette, M. G., Levit, M., and Park, P. (1995) in *Two-Component Signal Transduction* (Hoch, J. A., & Silhavy, T. J. Eds.) pp 25−51, ASM Press, Washington, DC.
2. Saraste, M., Sibbald, P. R., and Wittinghofer, A. (1990) *Trends Biochem. Sci.* 430−434.
3. Wierenga, R. K., Terpstra, P., and Hol, W. G. J. (1986) *J. Mol. Biol. 187*, 101−107.
4. Walker, J. E., Saraste, M., Runswick, M. J., and Gay, N. J. (1982) *Biochemistry 30*, 3834−3840.
5. Trach, K. A., and Hoch, J. A. (1993) *Mol. Microbiol. 8*, 69−79.
6. Wang, L., Grau, R., Perego, M., and Hoch, J. A. (1997) *Genes Dev.* (in press).
7. Ohlsen, K. L., Grimsley, J. K., and Hoch, J. A. (1994) *Proc. Natl. Acad. Sci. U.S.A. 91*, 1756−1760.
8. Perego, M., Hanstein, C. G., Welsh, K. M., Djavakhishvili, T., Glaser, P., and Hoch, J. A. (1994) *Cell 79*, 1047−1055.

9. Perego, M., and Hoch, J. A. (1996) *Proc. Natl. Acad. Sci. U.S.A. 93*, 1549−1553.
10. Perego, M., Glaser, P., and Hoch, J. A. (1996) *Mol. Microbiol. 19*, 1151−1157.
11. Perego, M. (1997) *Proc. Natl. Acad. Sci. U.S.A. 94*, 8612−8617.
12. Hoch, J. A. (1993) *Annu. Rev. Microbiol. 47*, 441−465.
13. Burbulys, D., Trach, K. A., and Hoch, J. A. (1991) *Cell 64*, 545−552.
14. Fisher, S. L., Kim, S.-K., Wanner, B. L., and Walsh, C. T. (1996) *Biochemistry 35*, 4732−4740.
15. Tawa, P., and Stewart, R. C. (1994) *Biochemistry 33*, 7917−7924.
16. Surette, M. G., Levit, M., Liu, Y., Lukat, G., Ninfa, E. G., Ninfa, A., and Stock, J. B. (1996) *J. Biol. Chem. 271*, 939−945.
17. Levit, M., Liu, Y., Surette, M., and Stock, J. B. (1996) *J. Biol. Chem. 271*, 32057−32063.
18. Stewart, R. C. (1997) *Biochemistry 36*, 2030−2040.
19. Zapf, J. W., Hoch, J. A., and Whiteley, J. M. (1996) *Biochemistry 35*, 2926−2933.
20. Zhou, X. Z., Madhusudan, Whiteley, J. M., Hoch, J. A., and Varughese, K. I. (1997) *Proteins 27*, 597−600.
21. Grimsley, J. K., Tjalkens, R. B., Strauch, M. A., Bird, T. H., Spiegelman, G. B., Hostomsky, Z., Whiteley, J. M., and Hoch, J. A. (1994) *J. Biol. Chem. 269*, 16977−16982.
22. Bradford, M. M. (1976) *Anal. Biochem. 72*, 248−254.
23. Laemmli, U. K. (1970) *Nature 227*, 680−685.
24. Lowry, O. H., and Passonneau, J. V. (1972) *A Flexible System of Enzymatic Analysis*, pp 147−149, Academic Press, New York.
25. Wilkinson, G. N. (1961) *Biochem. J. 80*, 324−332.
26. Cleland, W. W. (1979) in *Methods in Enzymology* (Purich, D. L. Ed.) Vol. 63, pp 103−138, Academic Press, San Diego.
27. Cleland, W. W. (1963) *Biochim. Biophys Acta 67*, 104−137.
28. Perego, M., Cole, S. P., Burbulys, D., Trach, K., and Hoch, J. A. (1989) *J. Bacteriol. 171*, 6187−6196.
29. Feher, V. A., Zapf, J. W., Hoch, J. A., Dahlquist, F. W., Whiteley, J. M., and Cavanagh, J. (1995) *Protein Sci. 4*, 1801−1814.
30. Neet, K. E. (1983) *Contemporary Enzyme Kinetics*, pp 267−320, Academic Press, New York.
31. Newton, A. C., and Koshland, D. E. (1987) *J. Biol. Chem. 262*, 10185−10188.
32. Todhunter, J. A., and Purich, D. L. (1977) *Biochim. Biophys. Acta 485*, 87−94.
33. Huang, K.-P., Chan, F.-F. J., Singh, T. J., Nakabayashi, H., and Huang, F. L. (1986) *J. Biol. Chem. 261*, 12134−12140.
34. Yang, Y., and Inouye, M. (1991) *Proc. Natl. Acad. Sci. U.S.A. 88*, 11057−11061.
35. Ninfa, E. G., Atkinson, M. R., Kamberov, E. S., and Ninfa, A. J. (1993) *J. Bacteriol. 175*, 7024−7032.
36. Morrison, J. F. (1979) *Methods Enzymol. 63*, 257−293.
37. Lukat, G. S., Stock, A. M., and Stock, J. B. (1990) *Biochemistry 29*, 5436−5442.
38. Parkinson, J. S., and Kofoid, E. C. (1992) *Annu. Rev. Genet. 26*, 71−112.
39. Bridger, W. A., Millen, W. A., and Boyer, P. D. (1968) *Biochemistry 8*, 3608−3615.
40. Wolodko, W. T., Brownie, E. R., O'Connor, M. D., and Bridger, W. A. (1983) *J. Biol. Chem. 258*, 14116−14119.
41. Bourret, R. B., Hess, J. F., and Simon, M. I. (1990) *Proc. Natl. Acad. Sci. U.S.A. 87*, 41−45.
42. Brissette, R. E., Tsung, K. L., and Inouye, M. (1991) *J. Bacteriol. 173*, 3749−3755.
43. Ferrari, F. A., Trach, K., LeCoq, D., Spence, J., Ferrari, E., and Hoch, J. A. (1985) *Proc. Natl. Acad. Sci. U.S.A. 82*, 2647−2651.
44. Trach, K., Chapman, J. W., Piggot, P. J., and Hoch, J. A. (1985) *Proc. Natl. Acad. Sci. U.S.A. 82*, 7260−7264.
45. Spiegelman, G., Van Hoy, B., Perego, M., Day, J., Trach, K., and Hoch, J. A. (1990) *J. Bacteriol. 172*, 5011−5019.


BI971917M